Despeckling Of Synthetic Aperture Radar Images Using Shearlet Transform

Anshika GOEL[1], *Amit GARG*[2]

[1]National Brain Research Centre, Manesar, Gurgaon, Haryana, India
[2]Department of Electronics and Communication Engineering, Ajay Kumar Garg Engineering College, Ghaziabad, Uttar Pradesh, India

anshika1508@gmail.com, amitstp@gmail.com

DOI: 10.15598/aeee.v21i3.4814

Article history: Received Nov 03, 2022; Revised Feb 15, 2023; Accepted Jul 10, 2023; Published Sep 30, 2023.

Abstract. *Synthetic Aperture Radar (SAR) is widely used for producing high quality imaging of Earth surface due to its capability of image acquisition in all-weather conditions. However, one limitation of SAR image is that image textures and fine details are usually contaminated with multiplicative granular noise named as speckle noise. This paper presents a speckle reduction technique for SAR images based on statistical modelling of detail band shearlet coefficients (SC) in homomorphic environment. Modelling of SC corresponding to noiseless SAR image are carried out as Normal Inverse Gaussian (NIG) distribution while speckle noise SC are modelled as Gaussian distribution. These SC are segmented as heterogeneous, strongly heterogeneous and homogeneous regions depending upon the local statistics of images. Then maximum a posteriori (MAP) estimation is employed over SC that belong to homogenous and heterogenous region category. The performance of proposed method is compared with seven other methods based on objective and subjective quality measures. PSNR and SSIM metrics are used for objective assessment of synthetic images and ENL metric is used for real SAR images. Subjective assessment is carried out by visualizing denoised images obtained from various methods. The comparative result analysis shows that for the proposed method, higher values of PSNR i.e. 26.08 dB, 25.39 dB and 23.82 dB and SSIM i.e. 0.81, 0.69 and 0.61 are obtained for Barbara image at noise variances 0.04, 0.1 and 0.15, respectively as compared to other methods. For other images also results obtained for proposed method are at higher side. Also, ENL for real SAR images show highest average value of 125.91 79.05. Hence, the proposed method signifies its potential in comparison to other seven existing image denoising methods in terms of speckle denoising and edge preservation.*

Keywords

NIG, shearlet transform, speckle noise, synthetic aperture radar.

1. Introduction

Synthetic aperture radar (SAR) is generally used to capture two-dimensional high-quality images of Earth surface in any weather conditions [1]. It provides useful information for a multitude of applications like land classification, tracking ships and mapping of forests. SAR continuously monitors the activities on earth surface efficiently. SAR images are captured by emitting the microwave signals from the remote sensor to the area of interest. This interaction between the target surface and remote sensor generates a multiplicative noise named as speckle noise. Speckle is a multiplicative granular noise present in SAR images [2]. It degrades the image resolution and effectiveness in visual interpretation. Hence, despeckling of SAR images is an important aspect in SAR image processing. In this work, a despeckling method for SAR images is presented which is capable of simultaneously suppressing speckle noise along with edge and texture preservation.

The reminder of the manuscript organization is as follows. Section 2. describes the related work in the area of SAR image denoising. Section 3. discusses about speckle noise and shearlet transform along with

detailed description of the methodology adopted for SAR image despeckling. Section 4. presents the experimental results evaluated over synthetic and real images along with comparison with current state of art methods. Finally, section 5. concludes the paper.

2. Related Work

Research for reducing speckle noise and to improve the visual effect of SAR images has been started four decades ago. Speckle reduction methods in SAR images can be applied in two ways i.e. before and after SAR image formation. The former approach includes multilook processing of SAR images, which reduces the speckle by taking the average of several statistically dependent looks of the same region in an image. This approach enhances the radiometric resolution but unfortunately reduces the spatial resolution when applied on SAR images [3]. To overcome this shortcoming, latter approach is preferred for SAR image despeckling. Post image despeckling methods can be classified as spatial domain and transform domain techniques. Former technique deal with direct manipulation of pixels or direct manipulation of reflectivity and speckle noise present in image [4]. A wide variety of spatial domain filters include Mean filter, Median filter, filters presented by Lee, Kuan and Frost. These methods produce good denoising results but the performance of these filters is compromised due to size and shape of filter used. Later non-local mean filters [5], [6] are proposed to overcome these limitations. Although, performance of these filters is good but computational burden is high. At present, hybrid filters are gaining prominence due to their capability of simultaneous edge retention and denoising. Hybrid filters are presented in [7]-[8]. Ali et. al. [7] presented a hybrid filter that is derived from a statistics filters having non-linear functions. In [8] a hybrid spatial domain filter based on coefficient of dispersion is presented. Transform domain filters provide an alternative method for speckle reduction in SAR images. A method based on fast Fourier transform for speckle noise reduction in SAR images is presented in [9]. The most common transform domain filters used for speckle reduction are filters based on discrete wavelet transform (DWT). But wavelet transform is not good in retaining directional edges in 2-D signals due to its discontinuity and singularity. For reducing shortcomings of wavelet transform, various other transforms have been introduced in the literature. Curvelets introduced by Candes and Donoho [10] shows good performance while working in continuous domain. However, in discrete domain performance of Curvelets is not satisfactory. Then contourlet transform is introduced by Do and Vitterli [11] which is entirely in discrete domain but is shift variant and not associated with multi-resolution analysis. Drawbacks of these transforms are overcome by Wang Q Lim's shearlet transform [12]. Shearlets are well localized with high directional sensitivity. Also, the approach is flexible which is helpful in image denoising. Speckle filtering in transform domain can further be categorized into thresholding and modelling based methods [13]. The performance of thresholding-based methods is dependent on the chosen threshold value based on which noise free SC are retained in subbands. Thresholding methods remove speckle in an efficient manner, but sometimes thresholding leads to the truncation of transform coefficients corresponding to signal and hence loss of information. Various thresholding-based denoising methods are presented in [14, 15, 16, 17, 18]. In [14] a combination of speckle reducing anisotropic filter and guided filter in wavelet domain is presented. Singh et. al. [15] proposed a homomorphic scheme using anisotropic diffusion in wavelet domain. In this scheme, approximation band coefficients are filtered with median filter while detailed band coefficients with soft thresholding method. Prabhishek et. al. [16] presented a hybrid method which combines directional smoothing filter along with wavelet thresholding approach. Sivaranjani et. al. [17] presented a method for calculating optimal threshold value in multi-objective particle swarm optimization framework using dual tree complex wavelet transform. Jain et. al. [18] formulates a novel thresholding function for speckle noise reduction. The proposed thresholding function is the modification of traditional soft thresholding function and is capable of preserving edges along with denoising.

However, modelling based methods are more useful as noise free coefficients are obtained using statistical modelling of transformed coefficients using suitable priors. These methods are capable of removing noise efficiently while preserving the edges and line structures of denoised images. The goal of modelling-based methods is to choose a precise prior model of noise free data on the basis of statistical knowledge. Li et. al. [19] proposed a denoising method which restores the speckle statistical characteristics along with denoising. Firstly a suitable priori is chosen for homogeneous region and then distribution parameters are estimated based on the value of pixels in these regions. Morteza et. al. [20] proposed a method based on non subsampled shearlet transform (NSST). NSST coefficients are modelled as t-location scale and denoised images are obtained using minimum mean squared error (MMSE) estimator. Yu et. al. [21] proposed a three step patch based method for speckle denoising. A new paradigm is proposed by Aksoy et. al. [22] in which both multiplicative and additive noise components of speckle noise are taken into consideration for the derivation of cost function. In literature, noise free transformed coefficients have been modelled using two sided generalized Gamma [23], Cauchy using stationary wavelet transform (SWT) [24], Cauchy using DWT [25], Nakagami

[26] and Weibull [27] distributions. However, Gaussian [2] and Rayleigh [28] distributions have been used for modelling of transformed coefficients corresponding to speckle noise.

In this work, a new transform domain approach based on the modelling of SC is presented for SAR image despeckling. Normal inverse Gaussian (NIG) is chosen for the modelling of noise free transformed coefficients, as these coefficients in SAR images can be well approximated by NIG distribution due to their heavy tailed data distribution. The main contribution of the work presented in this paper is that the SC in the detailed subbands are firstly divided into various regions viz., heterogeneous, strongly heterogeneous and homogeneous regions. A weight function 'Q' is defined and calculated for heterogeneous and homogeneous region SC. For controlling over smoothing during denoising process SC that lies in strongly heterogeneous regions are retained and not undergone for denoising process. Then, a MAP estimator is designed for the estimation of noise- free coefficients from the noisy data.

3. Materials and Methods

3.1. Speckle Noise

SAR images are degraded with both speckle noise and additive noise. Speckle noise is always present in SAR image and degrades image quality more harshly as compared to additive noise. SAR image model [8] can be expressed by Eq. (1).

$$y(a,b) = x(a,b).n(a,b), \tag{1}$$

x, y and n represent the noise free image, noisy image and speckle noise, respectively. For simplification, multiplicative noise is converted to additive noise using homomorphic filtering as expressed in Eq. (2).

$$y'(a,b) = x'(a,b) + n'(a,b), \tag{2}$$

Here, y', x' and n' are the logarithm transform of y, x and n, respectively.

3.2. Shearlet Transform

The limitation of sparse approximation and directionality of wavelets is overcome by shearlet. Shearlets are better in representing edges in images as compared to wavelets which are effective in handling only point discontinuities [29]. Shearlet transform is the combination of Laplacian Pyramid (LP) and the shear filter (SF) [12]. For representing multiple directions, shearlet transform uses a parabolic scaling matrix $A_{\alpha,2^j}$ as represented in Eq. (3), where $\alpha \in (0,2)$ is used for the measurement of the degree of anisotropy and $j \in \mathrm{Z}$ is the scaling parameter. The resolution of generating function is changed by parabolic scaling matrix. Shear matrix, S_k represented in Eq. (3) is designed for changing orientation of the generating function [30].

$$A_{\alpha,2^j} = \begin{bmatrix} 2^j & 0 \\ 0 & 2^{\alpha j/2} \end{bmatrix} and S_k = \begin{bmatrix} 1 & k \\ 0 & 1 \end{bmatrix}, \tag{3}$$

Assuming $f_j \in 1^2(Z^2)$ as scaling coefficient, the discrete shearlet transform is illustrated in Eq. (4),

$$DST^{2D}_{j,k,m}(f_J) = \left(\overline{\psi^d_{j,k}} * f_J\right)\left(2^J A^{-1}_{d^j} M_{c_j} m\right), \quad \text{for}: \ j = 0 \ldots J-1, \tag{4}$$

where

$$\psi^d_{j,k} = S^d_{k/2^{j/2}}\left(p_j * W_j\right), \tag{5}$$

$\psi^d_{j,k}$ is a support function, p_j is Fourier coefficients of 2-D fan filter. Sampling matrix M_{c_j} is selected such that $2^j A^{-1}_{2^j} M_{c_j} m$. Where, $m \in Z^2$ is the positive index.

Shearing operators are defined using Eq. (6) and Eq. (7) [30].

$$\overline{f_J} = \left((f_J)_{\uparrow 2^{j/2} *_1} h_{j/2}\right), \tag{6}$$

$$S^d_{2^{-j/2}k}(f_J) = \left(\left(\left(\overline{f_J}\right)(S_k \times)\right) *_1 \overline{h}_{j/2}\right)_{2^{j/2}}, \tag{7}$$

Where, $\overline{f_J}$ is the interpolated sampled values and $S_{2^{-j/2}k}$ is the shear operator. Shearlet system is the directional representation system providing sparse approximation of anisotropic features.

3.3. Inverse Shearlet Transform

Inverse shearlet transform (IST) can be obtained from ST using a frame reconstruction algorithm which is based on the conjugate gradient method. In the parabolic situation, the ST is simply a 2D convolution with shearlet filters which yield a linear shift-invariant transform [30]. Hence, ST takes the form

$$DST^{2(f_J)}_{j,k,m} = f_J * \bar{\psi}^d_{j,k}(m), \tag{8}$$

By switching the variable order digital shearlet filters $\tilde{\psi}^d_{j,k}$ corresponding to $\tilde{\psi}_{j,k,m}$ can be derived.

$$\widetilde{DST}^{2D}_{j,k,m} = f_J * \bar{\tilde{\psi}}^d_{j,k}(m), \tag{9}$$

The reconstruction formula for IST can be given by [30]

$$f_J = (f_J * \bar{\varphi}^d) * \phi^d + \sum_{j=0}^{J-1} \sum_{|k| \leqslant 2^{\lceil j/2 \rceil}} (DST^{2D}_{j,k,m}(f_J)) * \gamma^d_{j,k} + \sum_{j=0}^{J-1} \sum_{|k| \leqslant 2^{\lceil j/2 \rceil}} (DST^{2\hat{D}}_{j,k,m}(f_J)) * \tilde{\gamma}^d_{j,k}, \tag{10}$$

$$\overset{d}{\widehat{\psi}}(\xi) = |\overset{d}{\widehat{\varphi}}(\xi)|^2 + \sum_{j=0}^{J-1} \sum_{|k| \leqslant 2^{\lceil j/2 \rceil}} \left(|\overset{d}{\widehat{\psi}}_{j,k}(\xi)|^2 + |\overset{d}{\widehat{\tilde{\psi}}}_{j,k}(\xi)|^2 \right), \quad (11)$$

where

$$\gamma^d_{j,k}(\xi) = \frac{\psi^d_{j,k}(\xi)}{\overset{d}{\widehat{\psi}}(\xi)} \quad \text{and} \quad \tilde{\gamma}^d_{j,k}(\xi) = \frac{\psi^d_{j,k}(\xi)}{\overset{d}{\widehat{\psi}}(\xi)} \quad (12)$$

The expression for

$$\overset{d}{\widehat{\psi}}(\xi) = |\overset{d}{\widehat{\varphi}}(\xi)|^2 + \sum_{j=0}^{J-1} \sum_{|k| \leqslant 2^{\lceil j/2 \rceil}} \left(|\overset{d}{\widehat{\psi}}_{j,k}(\xi)|^2 + |\overset{d}{\widehat{\tilde{\psi}}}_{j,k}(\xi)|^2 \right) \quad (13)$$

Where, $\psi \in \mathbb{R}$ and ξ^d is called as the frame space. $\bar{\varphi}_d$ and $\widehat{\varphi}_d$ are sufficiently smooth scaling function and $\overset{d}{\widehat{\psi}}_{j,k}$ and $\overset{d}{\widehat{\tilde{\psi}}}_{j,k}$ are supporting functions with sufficient vanishing moments.

3.4. Modelling of Shearlet Coefficients

The prior distribution chosen for modelling noise free SC required a sharp peak with heavy tails. Hence, NIG distribution is used as a prior model for noise free SC and Gaussian distribution (GD) for speckle noise. For the validation of prior assumptions of the model, goodness of fit test is employed over noise free and noisy SC. Fig. 1(a) illustrates a plot between histogram of noisy data of Barbara image (20th detail shearlet sub-band) with GD. It can be seen easily that GD is perfectly matched with histogram data for noisy SC and hence is modelled as GD. The probability density function (PDF) of NIG distribution and histogram of noise-free SC (20th detail shearlet sub-band) are presented Fig. 1(b). It is to be noted that histogram of noise-free SC is exactly matched with NIG distribution and hence noise free SC are modelled as NIG distribution.

The PDF of NIG distribution is given using the Eq. (14).

$$f_X(X) = A_1 \frac{K_1\left(\alpha\sqrt{\delta^2 + X^2}\right)}{\sqrt{\delta^2 + X^2}}, \quad (14)$$

where K_1 is order one modified Bessel function of the second kind. Where, δ is scale parameter which defines the spread of the PDF and α is used to control the shape of NIG distribution. Parameter A_1 can be expressed using Eq. (15).

$$A_1 = \frac{\alpha\delta exp(\delta\alpha)}{\pi}. \quad (15)$$

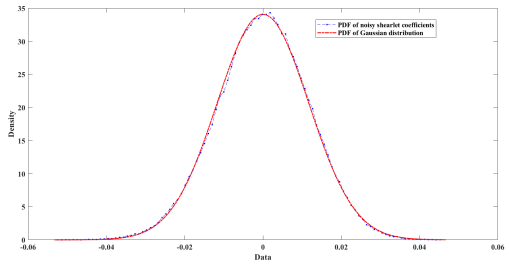

(a)

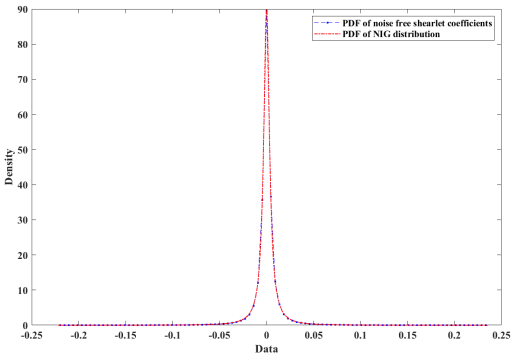

(b)

Fig. 1: (a) Histogram of noisy SC plotted with PDF of Gaussian distribution, (b) Histogram of noise-free SC plotted with PDF of NIG distribution.

3.5. Parameter Estimation and MAP Estimation

Shearlet coefficients for any arbitrary sub-band 'k' of log transformed image can be represented using Eq. (16).

$$Y^k = X^k + N^k, \quad (16)$$

Here, Y^k, X^k and N^k are the transformed coefficients of $y'(a,b)$, $x'(a,b)$ and $n'(a,b)$ respectively. For simplicity, subscript k is ignored, and hence Eq. (16) can be written as $Y = X + N$. For estimating noise free SC from the observed noisy SC, Bayesian MAP estimator is expressed in Eq. (17).

$$\hat{X} = \arg\max_X \left[f\left(X/Y\right) \right]. \quad (17)$$

Thus, from Bayes theorem,

$$\hat{X} = \arg\max_X \left[f\left(Y/X\right) f\left(X\right) \right] = \arg\max_X \left[f_N\left(Y - X\right) f_X\left(X\right) \right], \quad (18)$$

Here, $f_x(X)$ is the prior distribution assumed as NIG and $f_N(.)$ is the PDF of the noise. Because of log transformation applied on the noisy image the distribution is assumed as Gaussian. Thus, the PDF of noise can

be expressed using Eq. (19).

$$f_N(N) = \frac{1}{\sqrt{2\pi}\sigma_N} exp\left(-\frac{N^2}{2\sigma_N^2}\right). \quad (19)$$

Since $Ln(.)$ is monotone, Eq. (12) can be expressed as given in Eq. (20).

$$\hat{X} = \arg\max_X \left[Ln\left(f_N(Y-X)\right) + Ln\left(f_X(X)\right)\right]. \quad (20)$$

Substituting the values of prior distribution and noise PDF from Eq. (14) and Eq. (19) in Eq. (20), we have

$$\hat{X} = \arg\max_X \left[\frac{-(Y-X)^2}{2\sigma_N^2} + Ln\left(\frac{\alpha\delta exp(\delta\alpha)}{\pi}\frac{K_1\left(\alpha\sqrt{\delta^2+X^2}\right)}{\sqrt{\delta^2+X^2}},\right)\right] \quad (21)$$

$$\hat{X} = \arg\max_X \left[F(X)\right]. \quad (22)$$

As the above equation is not linear Eq. (22) can be written as from Hyvarinen's work [31].

$$\hat{X}_{NIG} = sign(Y)\max\left(0, |Y| - \sigma_N^2 |F'(Y)|\right), \quad (23)$$

Thus, estimated noise free shearlet coefficients of the transform can be reduced using Eq. (24). But to further enhance the despeckling capability, the above despeckling equation is modified using a weight function Q which helps in reducing the loss of feature information as shown in Eq. (25)

The heterogeneity function Q is defined in Eq. (26) [32]

$$Q = \exp\left\{-\frac{1}{\gamma}\left(\frac{R_Y}{R_Z} - 1\right)\right\}. \quad (26)$$

Parameter γ is tunable and can be chosen differently for different images. R_Z is a constant and is equal to

$$R_Z = \sqrt{S_z^k}\frac{\sigma_Z}{\mu_Z}. \quad (27)$$

Here, S_z^k is the equivalent high frequency response of the ST [32]. As to R_Y, it is calculated as

$$R_Y = \frac{\sigma_Y}{\mu}. \quad (28)$$

Here, σ_Y and μ are the local estimates of detailed sub-bands of shearlet transform and original image respectively. Local estimates are calculated using a neighborhood of size $D_j \times D_j$.

$$\sigma_Y(p,q) = \frac{1}{D_j x D_j}\sum_{k=-D_0}^{D_0}\sum_{l=-D_0}^{D_0} Y^k(p+k, q+l), \quad (29)$$

$$\mu(p,q) = \frac{1}{D_j x D_j}\sum_{k=-D_0}^{D_0}\sum_{l=-D_0}^{D_0} y(p+k, q+l). \quad (30)$$

Detail band SC are divided in different regions with the help of local statistics of the image.

- $R_Y \leqslant a_1 R_Z$

The current pixel is associated with homogeneous region. In the homogeneous regions of detailed band, $R_Y = R_Z$. Then, Q will equivalently be 1.

- $a_1 R_Z < R_Y < a_2 R_Z$

The pixel belongs to heterogeneous region. Thus, for each pixel the heterogeneous adaptive threshold Q changes.

- $R_Y \geqslant a_2 R_Z$

The pixel belongs to strongly heterogeneous class. This class includes the strong edges and point targets. Despeckling model is not valid for this class as speckle is not fully developed. Thus, values of SC of this class are preserved. Further, to solve the MAP equation, NIG distribution parameters for speckle free image are required. They can be estimated using absolute central moments and cumulants. The characteristic function of NIG PDF and the corresponding cumulant generating function are given by Eq. (31) and Eq. (32), respectively.

$$\varphi(\omega) = exp\left(\delta\alpha - \delta\sqrt{\alpha^2+\omega^2}\right) \quad (31)$$

$$C(\omega) = \ln\varphi(\omega) = \delta\alpha - \delta\sqrt{\alpha^2+\omega^2}. \quad (32)$$

Thus, the cumulants can be obtained with the help of cumulant generating function, using Eq. (33).

$$k_n = (-j)^n \frac{\partial C(\omega)}{\partial\omega}. \quad (33)$$

Thus, second order and fourth order cumulants are obtained by

$$k_2 = \frac{\delta}{\alpha}, \quad (34)$$

$$k_4 = \frac{3\delta}{\alpha^3} \quad (35)$$

The values of second and fourth order moments are calculated using empirical data Y with the help of DxD

$$\hat{X}_{NIG} = sign\,(Y) \max\left(0, |Y| - \sigma_N^2 \left| \frac{2Y}{\delta^2 + Y^2} + \frac{\alpha Y}{\sqrt{\delta^2 + Y^2}} \frac{K_0\left(\alpha\sqrt{\delta^2 + Y^2}\right)}{K_1\left(\alpha\sqrt{\delta^2 + Y^2}\right)} \right| \right). \quad (24)$$

$$\hat{X}_{NIG} = sign\,(Y) \max\left(0, |Y| - \sigma_N^2 Q \left| \frac{2Y}{\delta^2 + Y^2} + \frac{\alpha Y}{\sqrt{\delta^2 + Y^2}} \frac{K_0\left(\alpha\sqrt{\delta^2 + Y^2}\right)}{K_1\left(\alpha\sqrt{\delta^2 + Y^2}\right)} \right| \right). \quad (25)$$

window. The respective values are given by

$$m_2^Y(k,l) = \frac{1}{D^2} \sum_{i=-M/2}^{M/2} \sum_{j=-M/2}^{M/2} Y(k-i, l-j)^2, \quad (36)$$

$$m_4^Y(k,l) = \frac{1}{D^2} \sum_{i=-M/2}^{M/2} \sum_{j=-M/2}^{M/2} Y(k-i, l-j)^4. \quad (37)$$

The corresponding coefficients of noise free data can be obtained using

$$m_2^X(k,l) = \max\left(\left(m_2^Y(k,l) - \sigma_N^2\right), 0\right), \quad (38)$$

$$m_4^X(k,l) = \max\left(\left(m_4^Y(k,l) - 6m_2^X(k,l)\,\sigma_N^2 - 3\sigma_N^4\right), 0\right). \quad (39)$$

Now the corresponding second and fourth order cumulants are presented by

$$\bar{k}_2 = m_2^X, \quad (40)$$

$$\bar{k}_4 = \max\left(\left(m_4^X - 3\left(m_2^X\right)^2\right), 0\right). \quad (41)$$

Thus, substituting the value of cumulants in Eq. (34) and (35), the corresponding parameters of NIG distribution can be estimated.

3.6. Proposed Despeckling Algorithm

The block diagram of proposed despeckling technique is illustrated in Fig. 2. Initially, speckled image is taken and log transformation is applied on it. Then shearlet decomposition is carried out for 3-levels resulting in 32 detail subbands and 1 approximation subband. Then accomplish the following procedures on each detailed shearlet sub-band coefficients:

- **Pixel Classification**: Calculate R_Y and R_Z. If pixel belongs to homogenous or heterogeneous class, calculate Q.
- **Parameter Estimation**: Calculate parameter α and δ with the help of moments and cumulants.
- **Bayesian MAP estimation**: Estimate denoised shearlet coefficients for homogenous and heterogeneous class with the help of Bayesian MAP equation. Shearlet coefficients corresponding to highly heterogeneous class remains the same.

Then perform inverse shearlet transform (IST) on despeckled SC to obtain the noise free log compressed image. Then final denoise image of better quality is obtained after applying exponential operator to log compressed denoised image.

4. Experimental Results

Despeckling experiments were performed on synthetic images and real SAR images. Standard gray scale synthetic images of different textures are chosen to assess the efficacy of proposed method. Real SAR images were taken from Sandia Laboratories (https://www.sandia.gov/radar/pathfinder-radar-isr-and-synthetic-aperture-radar-sar-systems/complex-data/) [33]. The performance of proposed method is evaluated and compared with seven existing techniques, viz. thresholding of contourlet transform [11], SWT modeling using Cauchy distribution [24], SWT modeling using generalized gamma distribution (GΓD) [3], DWT modeling using Cauchy distribution [25], hybrid filter proposed by Ali et. al. [7], thresholding method presented by Jain et. al. [18] and modelling method proposed by Morteza et. al. [20]. Efficiency of denoising technique for synthetic image is measure using reference image quality metric, peak signal to noise ratio (PSNR) [1] and structural similarity index measure (SSIM) [34]. A higher PSNR specifies a high- quality image. SSIM computes the degree of similarity between two images. Measurement of the image quality depends on a reference image which is an uncompressed or distortion-free image. The value of SSIM always lies between 0 and 1. If the value of SSIM is close to 1, then the resulting image is similar to original image. However, equivalent number of looks (ENL) [15] is used to assess the objective quality of real images. ENL is computed for a local

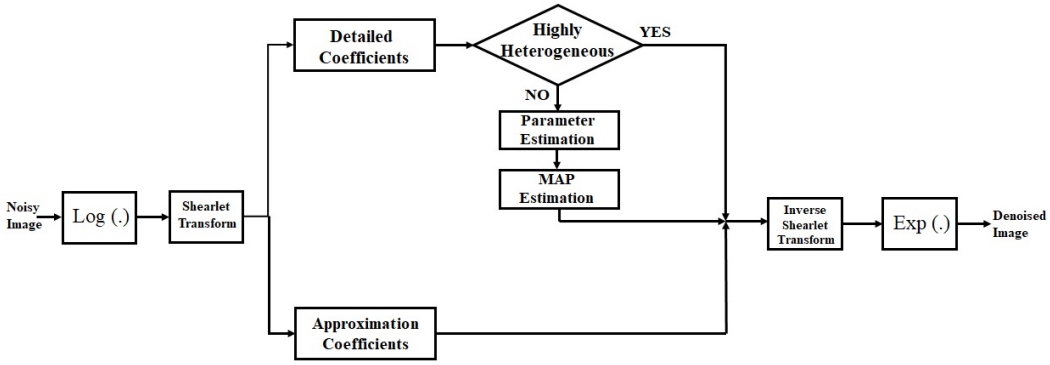

Fig. 2: Block diagram of proposed despeckling method.

Tab. 1: Comparison Table for PSNR values on different synthetic images.

Image	Speckle Noise Variance	PSNR								
		Noisy Image	Contourlet [11]	SWT_Cauchy [24]	SWT_GΓD [3]	DWT_Cauchy [25]	Hybrid [7]	Thresholding [18]	Modelling [20]	Proposed Method
Barbara	0.04	20.06	24.95	22.95	25.99	25.67	23.05	26.01	26.05	26.08
	0.1	16.34	22.27	18.89	22.85	23.83	18.99	24.93	25.36	25.39
	0.15	14.73	20.75	16.83	22.24	21.87	17.96	22.82	23.72	23.82
Baboon	0.04	19.47	21.86	21.92	23.96	22.90	22.89	23.95	23.92	23.98
	0.1	15.69	20.07	18.38	21.48	21.47	21.41	22.38	22.36	22.41
	0.15	14.09	19.04	16.01	20.69	20.73	16.05	21.34	21.38	21.46
House	0.04	21.46	21.72	21.88	22.01	22.76	21.78	23.99	24.03	24.12
	0.1	17.74	19.93	18.47	20.67	21.73	18.42	22.01	22.04	22.15
	0.15	16.14	19.06	15.84	19.67	19.98	15.79	20.87	21.60	21.61
Cameraman	0.04	19.59	24.09	21.23	24.45	24.74	21.24	25.34	25.12	25.73
	0.10	15.74	21.77	18.55	22.72	23.72	18.58	24.03	24.08	24.32
	0.15	14.16	20.40	16.58	19.89	22.68	16.61	23.16	23.17	23.52

homogeneous region and it is the ratio of square of mean to the variance of that region.

4.1. Experiments on synthetic images

Standard gray scale images; Barbara, Baboon, House and Cameraman were taken to assess the efficiency of the proposed despeckling method. Corresponding noisy images are generated by inbuilt function 'imnoise' available in MATLAB. This function generates the noisy image from original image by adding random noise of zero mean and variance as specified in function. Table 1 and Table 2 show the PSNR and SSIM values, respectively for standard synthetic images; Barbara, Baboon, House and Cameraman for proposed and existing despeckling methods. For implementation of contourlet method [11] wavelet transform with "9-7" biorthogonal filters and six level of decomposition is used. For implementing SWT modelling using Cauchy [24] "Symlet" wavelet of order 8 with four level of decomposition is used. For the implementation of both SWT-GΓD [3] and DWT-Cauchy [25], 'db4' wavelet with three levels of wavelet decomposition is used. For hybrid filter [7] local window size for both mean and median filter is taken as 3x3 and the value of control factors a1 and a2 are taken as 0.02 and 0.12, respectively. For thresholding method [18] 'db8' wavelet with two levels of decomposition is used and the value of threshold 'T' used in evaluating proposed thresholding function is calculated using Bayes Shrink method. In modelling method [20] for NSST coefficients three levels of decomposition is chosen and MMSE criterion is used for obtaining denoised images. For the implementation of proposed method three levels of ST coefficients are used. The value of parameters a1 and a2 are chosen as 1 and 5, respectively and local window of size 5x5 is chosen for all the experimentation. All these parameters are used for all the images used in the experimentation.

PSNR and SSIM values are obtained for NV, 0.04, 0.1 and 0.15. It can be observed from Table 1 and Table 2 that the proposed method has better PSNR and SSIM values in comparison to the existing methods. Figure 3 represents the images for visual quality evaluation of synthetic image, Barbara. Fig. 3(a) represents the noisy image with NV 0.1. Figure 3(b) shows the denoised image obtained from contourlet thresholding method. Denoised image obtained from this method gives overly smoothed region but the edges are blurred in these regions. Figure 3(c) and Fig. 3(d) show de-

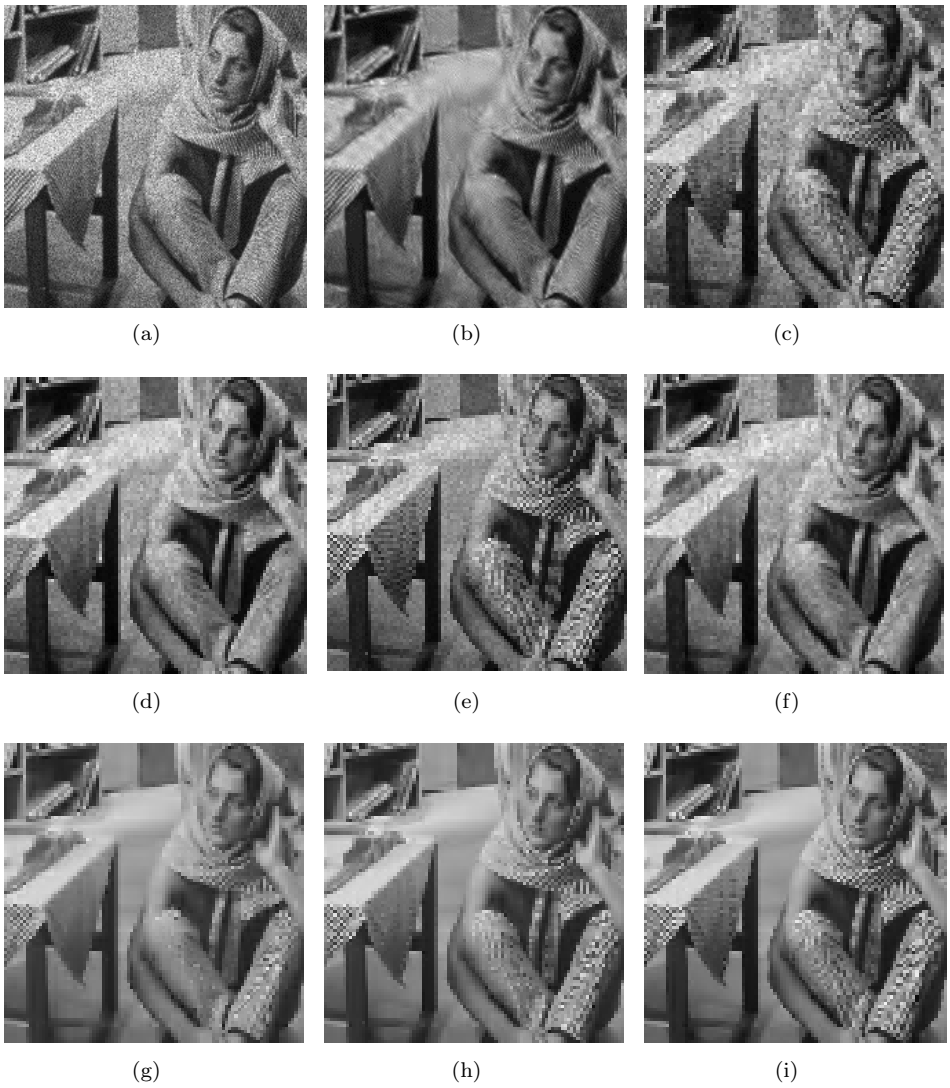

(a) (b) (c)

(d) (e) (f)

(g) (h) (i)

Fig. 3: Synthetic Barbara images obtained for various despeckling methods, (a) Noisy image (NV =0.1), (b) Contourlet, (c) SWT_Cauchy, (d) SWT_GΓD, (e) DWT-Cauchy, (f) Hybrid, (g) Thresholding, (h) Modelling, (i) Proposed.

(a) (b)

Fig. 4: ENL calculations for region highlighted in red, (a) Real Image 1, (b) Real Image 2.

Tab. 2: Comparison Table for SSIM values on different synthetic images.

Image	Speckle Noise Variance	SSIM								
		Noisy Image	Contourlet [11]	SWT_Cauchy [24]	SWT_GΓD [3]	DWT_Cauchy [25]	Hybrid [7]	Thresholding [18]	Modelling [20]	Proposed Method
Barbara	0.04	0.47	0.71	0.64	0.73	0.76	0.59	0.79	0.81	0.81
	0.1	0.32	0.61	0.48	0.62	0.63	0.44	0.68	0.65	0.69
	0.15	0.26	0.54	0.40	0.57	0.55	0.37	0.60	0.59	0.61
Baboon	0.04	0.53	0.55	0.61	0.64	0.59	0.60	0.61	0.63	0.65
	0.1	0.37	0.42	0.49	0.53	0.52	0.43	0.54	0.52	0.55
	0.15	0.30	0.36	0.42	0.46	0.43	0.41	0.39	0.45	0.48
House	0.04	0.50	0.58	0.73	0.63	0.69	0.64	0.69	0.73	0.74
	0.1	0.46	0.48	0.61	0.58	0.59	0.55	0.58	0.60	0.63
	0.15	0.39	0.43	0.53	0.55	0.52	0.51	0.52	0.55	0.57
Cameraman	0.04	0.44	0.63	0.57	0.65	0.66	0.51	0.67	0.72	0.75
	0.1	0.35	0.55	0.45	0.54	0.54	0.44	0.53	0.61	0.63
	0.15	0.30	0.51	0.39	0.51	0.44	0.37	0.47	0.55	0.56

Tab. 3: ENL values for real SAR images.

Image	Image Region	SSIM							
		Contourlet [11]	SWT_Cauchy [24]	SWT_GΓD [3]	DWT_Cauchy [25]	Hybrid [7]	Thresholding [18]	Modelling [20]	Proposed Method
Real Image 1	Region 1	39.35	38.99	39.12	39.23	38.96	39.46	40.12	41.77
	Region 2	43.82	45.61	65.97	65.67	45.58	66.98	66.35	67.80
Real Image 2	Region 1	83.77	67.58	197.4	189.36	93.25	243.12	244.27	249.45
	Region 2	146.35	133.30	144.72	155.79	135.95	167.12	172.36	179.45

speckled images obtained from modelling of SWT coefficients using Cauchy and generalized gamma distributions, respectively. A different type of pattern is seen in these images as speckle noise is removed effectively, but the image edges got blurred and small details are masked. The quality of the image obtained using hybrid method (Fig. 3(f)) is almost similar to the one obtained using SWT-Cauchy (Fig. 3(c)) method but inferior to the one obtained using SWT-GΓD (Fig. 3(d)) and DWT-Cauchy (Fig. 3(e)) method. Figure 3(g) and Fig. 3(h) represent the denoised images obtained using thresholding method and modelling methods, respectively. The denoised image obtained using modelling method is better than the one obtained using thresholding method but inferior to the one obtained using proposed method. Figure 3(i) shows the denoised image obtained from proposed method. It can be seen that proposed method suppresses the speckle noise in most effective manner while retaining important image details.

4.2. Experiments on real SAR images

For quantitative assessment of real SAR images, a non-reference parameter ENL is measured due to unavailability of noise free real SAR images. ENL is calculated on homogenous area of the image for evaluating the performance of real images. Figure 4 shows two real SAR images with two homogenous regions in each image. These regions are shown by rectangles of red colour boundary on images. Table 3 shows the ENL values obtained for four regions corresponding to two real images for existing as well as proposed method. ENL values evaluated for proposed method is greater than the one obtained for existing methods. Thus, our proposed method outperforms other compared methods. For subjective assessment, despeckling results of existing and proposed method have been presented in Fig. 5. Figure 5(a)- Figure 5(i) illustrate denoised images obtained from all methods under consideration for Real image 1. After visual quality inspection of denoised images it is found that the image obtained using proposed method is superior to all other images. Also, it can be perceived that noise has been eliminated effectively while details are not lost in the denoised image using proposed scheme.

Moreover, for further testing the efficacy of the proposed scheme, results have been carried out on 30 real SAR images for 60 homogenous regions. Table 4 shows the average ENL values along with standard deviation obtained for 60 regions of 30 real images for existing as well as proposed method. It is to be noted that average ENL value for proposed scheme as compared to other schemes is at higher side.

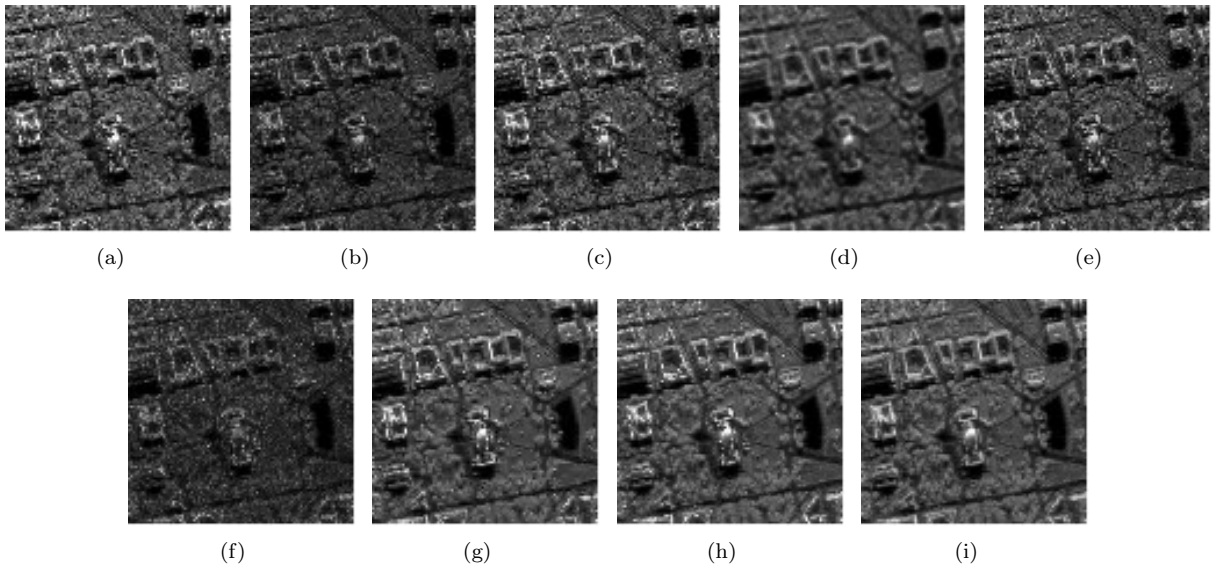

Fig. 5: Despeckled real Image 1 obtained from various despeckling methods(a) Noisy image, (b) Contourlet, (c) SWT_Cauchy, (d) SWT_GΓD, (e) DWT-Cauchy, (f) Hybrid, (g) Thresholding, (h) Modelling, (i) Proposed.

Tab. 4: Average ENL values for thirty real SAR images.

Method	Mean SD
Contourlet [11]	70.74 ± 40.83
SWT-Cauchy [24]	65.08 ± 34.84
SWT-GΓD [3]	99.58 ± 63.12
DWT-Cauchy [25]	106.25 ± 41.31
Hybrid [7]	95.36 ± 35.12
Thresholding [18]	108.29 ± 32.18
Modelling [20]	115.23 ± 67.89
Proposed Method	125.91 ± 79.05

5. Conclusion

A new speckle reduction scheme based on modelling of detailed band SC is proposed in this work. Noise free shearlet coefficients are estimated by taking NIG distribution as a prior. MAP estimation criterion is carried out for estimating the noise free SC. Objective and subjective results are presented for synthetic images and for real SAR images. PSNR and SSIM parameters for synthetic images and non-reference measure, ENL is computed on real images. The proposed method is showing superior performance because of using of ST which provides directional sensitivity due to which edges of the images are optimally modelled. Also, another advantage is that to avoid oversmoothing, SC corresponding to strongly heterogeneous regions are retained due to which edge preservation is better. Objective evaluation metrics PSNR, SSIM and ENL confirms that the proposed method is superior to other existing methods. Also, from subjective quality evaluation it is evident that the images obtained using proposed method is the best in terms of denoising and edge preservation. Hence, the proposed despeckling scheme is a potential scheme for speckle reduction along with preservation of important image details in SAR images. As a future scope MAP estimator can be designed by considering the statistical dependency of the SC. Also, modelling of SC using NIG can be used in another image processing applications such as image watermarking.

Acknowledgment

The authors would like to thank Ajay Kumar Garg Engineering College, Ghaziabad for providing the necessary research facilities.

Author Contributions

A. Goel and A. Garg both developed the idea and theoretical formalism. Both authors A. Garg and A. Goel performed analytic calculations and then performed simulation. A. Goel prepared the draft of manuscript and both authors contributed to the final version of manuscript.

References

[1] MOREIRA, A., P. PRATS-IRAOLA, M. YOUNIS, G. KRIEGER, I. HAJNSEK, and K.P. PAPATHANASSIOU. A tutorial on synthetic aperture radar. *IEEE Geoscience and remote sensing magazine*. 2013, vol. 1, iss. 1, pp. 6-43. ISSN 2168-6831. DOI: 10.1109/MGRS.2013.2248301.

[2] GOEL, A. and A. GARG,. Despeckling of SAR images using discrete shearlet transform. *In: International Conference on Information, Communication, Instrumentation and Control (ICICIC)*. Indore: IEEE, 2017, pp. 1-6. ISBN 978-1-5090-6313-0. DOI: 10.1109/ICOMICON.2017.8279165.

[3] CHEN, H., Y. ZHANG, H. WANG, and C. DING. Stationary-wavelet-based despeckling of SAR images using two-sided generalized gamma models. *IEEE Geoscience and Remote Sensing Letters*, 2012, vol. 9, iss. 6, p.p 1061-1065. ISSN 1558-0571. DOI: 10.1109/LGRS.2012.2189093.

[4] MURUGESAN, K., P. BALASUBRAMANI, and P.R. MURUGAN. A quantitative assessment of speckle noise reduction in SAR images using TLFFBP neural network. *Arabian Journal of Geosciences*, 2020, vol. 13, iss. 35, pp.1-17. ISSN 1866-7538. DOI: 10.1007/s12517-019-4900-4.

[5] CHAN, D., J. GAMBINI, and A.C. FRERY. Speckle noise reduction in SAR images using information theory. *In: Latin American GRSS & ISPRS Remote Sensing Conference (LAGIRS)*. Santiago, Chile, IEEE, 2020, pp. 456-461. ISBN:978-1-7281-4350-7 DOI: 10.1109/LAGIRS48042.2020.9165582.

[6] FERRAIOLI, G., V. PASCAZIO, and G. SCHIRINZI. Ratio-based nonlocal anisotropic despeckling approach for SAR images. *IEEE Transactions on Geoscience and Remote Sensing*, 2019, vol. 57, iss. 10, pp.7785-7798. ISSN 1558-0644. DOI: 10.1109/TGRS.2019.2916465.

[7] ALI, E.H., REJA, A.H. and L.H. ABOOD. Design hybrid filter technique for mixed noise reduction from synthetic aperture radar imagery. *Bulletin of Electrical Engineering and Informatics*, 2022, vol. 11, iss. 3, pp.1325-1331. ISSN 2089-3191. DOI: 10.11591/eei.v11i3.3708.

[8] GARG, A. and V. KHANDELWAL. Combination of Spatial Domain Filters for Speckle Noise Reduction in Ultrasound Medical Images. *Advances in Electrical and Electronic Engineering*. 2017, vol. 15, iss. 5, pp. 857-865. ISSN 1804-3119. DOI: 10.15598/aeee.v15i5.2288.

[9] SAPUTRO, A. and D. KUSHARDONO. Speckle noise reduction of Sentinel-1 SAR data using fast fourier transform temporal filtering to monitor paddy field area. *In IOP Conference Series: Earth and Environmental Science*. Bandar Lampung, Indonesia, 2021. p. 012086. ISSN 1755-1315. DOI: 10.1088/1755-1315/739/1/012086.

[10] STARCK, J.L., E.J. CANDÈS, and D.L. DONOHO. The curvelet transform for image denoising. *IEEE Transactions on image processing*. 2002, vol.11, iss. 6, pp. 670-684. ISSN 1941-0042. DOI: 10.1109/TIP.2002.1014998.

[11] DO, M.N. and M. VETTERLI. The contourlet transform: an efficient directional multiresolution image representation. *IEEE Transactions on image processing*. 2005, vol. 14, iss. 12, pp. 2091-2106. ISSN 1941-0042. DOI: 10.1109/TIP.2005.859376.

[12] LIM, W.Q. The discrete shearlet transform: A new directional transform and compactly supported shearlet frames. *IEEE Transactions on image processing*. 2010. vol. 19, iss. 5, pp. 1166-1180. ISSN 1941-0042. DOI: 10.1109/TIP.2010.2041410.

[13] GARG, A., V. KHANDELWAL. Despeckling of medical ultrasound images using fast bilateral filter and NeighShrinkSure filter in wavelet domain. In: Rawat, B., Trivedi, A., Manhas, S., Karwal, V. (eds) Advances in Signal Processing and Communication. *Lecture Notes in Electrical Engineering*, vol 526. Springer, Singapore 2019, pp. 271-280. ISBN 978-981-13-2553-3. DOI: 10.1007/978-981-13-2553-3_26.

[14] CHOI, H. and J. JEONG. Speckle noise reduction technique for SAR images using statistical characteristics of speckle noise and discrete wavelet transform. *Remote Sensing*. 2019. vol. 11, iss. 10. p. 1184. ISSN 20724292. DOI: 10.3390/rs11101184.

[15] SINGH, P. and R. SHREE. A new homomorphic and method noise thresholding based despeckling of SAR image using anisotropic diffusion. *Journal of King Saud University-Computer and Information Sciences*. 2020, vol. 32, iss. 1, pp. 137-148. ISSN 2213-1248. DOI: 10.1016/j.jksuci.2017.06.006.

[16] SINGH, P. and R. SHREE. A new SAR image despeckling using directional smoothing filter and method noise thresholding. *Engineering Science and Technology, an International Journal*. 2018, vol. 21, iss. 4, pp.589-610. ISSN 2215-0986. DOI: 10.1016/j.jestch.2018.05.009.

[17] SIVARANJANI, R., S.M.M ROOMI and M. SENTHILARASI. Speckle noise removal in SAR images using Multi-Objective PSO (MOPSO) algorithm. *Applied Soft Computing*. 2019, vol. 76, pp.671-681. ISSN 1872-9681. DOI: 10.1016/j.asoc.2018.12.030.

[18] JAIN, L. and P. SINGH. A novel wavelet thresholding rule for speckle reduction from ultrasound images. *Journal of King Saud University-Computer and Information Sciences*. 2022, vol. 34, iss. 7, pp. 4461-4471. ISSN 2213-1248. DOI: 10.1016/j.jksuci.2020.10.009.

[19] LI, Y., S. WANG, Q., ZHAO, and WANG, G. A new SAR image filter for preserving speckle statistical distribution. *Signal Processing*. 2020, vol. 176, p.107706. ISSN 1872-7557 DOI: 10.1016/j.sigpro.2020.107706.

[20] MORTEZA, A. and M. AMIRMAZLAGHANI. A novel statistical approach for multiplicative speckle removal using t-locations scale and non-sub sampled shearlet transform. *Digital Signal Processing*. 2020, vol. 107, p.102857. ISSN 1095-4333. DOI: 10.1016/j.dsp.2020.102857.

[21] YU, Z., W. WANG, C. LI, W. LIU, and J. YANG. Speckle noise suppression in SAR images using a three-step algorithm. *Sensors*, 2018, vol. 18, iss. 11, p.3643. ISSN 14243210. DOI: 10.3390/s18113643.

[22] AKSOY, G. and F. NAR. Multiplicative-additive despeckling in SAR images. *Turkish Journal of Electrical Engineering and Computer Sciences*. 2020, vol. 28, iss. 4, pp.1871-1885. ISSN 1303-6203. DOI: 10.3906/elk-1908-163.

[23] JAFARI, S., S.GHOFRANI. Using two coefficients modeling of nonsubsampled Shearlet transform for despeckling. *Journal of Applied Remote Sensing*. 2016. vol. 10, iss.1, pp.015002-1-015002-14. ISSN 1931-3195. DOI: 10.1117/1.JRS.10.015002.

[24] BHUIYAN, M. I. H., M. O. AHMAD and M. N. S. SWAMY. Spatially adaptive wavelet-based method using the Cauchy prior for denoising the SAR images. *IEEE Transactions on Circuits and Systems for Video Technology*. 2007, vol. 17, iss. 4, pp. 500-507. ISSN 1558-2205. DOI: 10.1109/TCSVT.2006.888020.

[25] SAHU, S., H.V. SINGH, B. KUMAR and A.K. SINGH. De-noising of ultrasound image using Bayesian approached heavy-tailed Cauchy distribution. *Multimedia Tools and Applications*. 2019. vol.78, iss. 4, pp. 4089-4106. ISSN 1573-7721. DOI: 10.1007/s11042-017-5221-9.

[26] GARG, A., and V.KHANDELWAL. Speckle noise reduction in medical ultrasound images using modelling of shearlet coefficients as a Nakagami prior. *Advances in Electrical and Electronic Engineering*. 2018, vol. 16, iss. 4, pp.538-549. ISBN 1804-3119. DOI: 10.15598/aeee.v16i4.2858.

[27] LIU, J., Z. TANG, P.XU, W.LIU,, J. ZHANG and J. ZHU. Quality-related monitoring and grading of granulated products by weibull-distribution modeling of visual images with semi-supervised learning. *Sensors*. 2016, vol. 16, iss. 7, pp. 998. ISSN 1424-8220. DOI: 10.3390/s16070998.

[28] BELOV, A.A., V.A. PAVLOV, and A.A. TUZOVA. A method of finding optimal parameters of speckle noise reduction filters. *In: Internet of Things, Smart Spaces, and Next Generation Networks and Systems*. Springer 2020, pp. 133-141. ISBN 978-3-030-65729-1 DOI: 10.1007/978-3-030-65729-1_12.

[29] EASLEY, G., LABATE, D. and W.Q. LIM,. Sparse directional image representations using the discrete shearlet transform. *Applied and Computational Harmonic Analysis*. 2008. vol. 25, iss. 1, pp. 25-46. ISSN 1063-5203. DOI: 10.1016/j.acha.2007.09.003.

[30] KUTYNIOK, G., W. LIM, and R.S. REISENHOFER. Shearlab 3D: Faithful Digital Shearlet Transforms based on Compactly Supported Shearlets. *ACM Transactions on Mathematical Software (TOMS)*. 2016, vol. 42, iss. 1, pp.1-42. ISSN 0098-3500. DOI: 10.1145/2740960.

[31] HYVÄRINEN, A. Sparse code shrinkage: denoising of non-gaussian data by maximum likelihood estimation. *Neural Computation*. 1999, vol. 11, iss. 7, pp. 1739-1768. ISSN 0899-7667. DOI: 10.1162/089976699300016214.

[32] FOUCHER, S., G.B. BÉNIÉ, and J.-M. BOUCHER. Wavelet filtering of SAR images based on non-Gaussian assumptions. *In: Proceedings of the International Conference on Acoustics, Speech and Signal Processing*, ICASSP'98.:IEEE, 1998, pp. 2925-2928. ISSN 1520-6149. DOI: 10.1109/ICASSP.1998.678138.

[33] SAR Image Database. In: Available at: `https://www.sandia.gov/radar/pathfinder-radar-isr-and-synthetic-aperture-radar-sar-systems/complex-data/`.

[34] Silvestre B, J., Structural similarity image quality reliability: Determining parameters and window size. *Signal Processing*. 2011. vol. 91, iss. 4, pp. 1012-1020. ISSN 0165-1684. DOI: 10.1016/j.sigpro.2010.10.003.

About Authors

Anshika GOEL was born in Sitapur, India. She received her M. Tech degree in Electronics and Communication Engineering from Ajay Kumar Garg Engineering College, Ghaziabad, India in 2008. She is currently working as Research Scientist at National Brain Research Centre, Gurgaon, India. Her research interests include medical imaging, signal processing, image processing and image denoising.

Amit GARG was born in Agra, India. He received his Ph.D from Jaypee Institute of Information Technology, Noida, India in area of image processing. He is currently working as Associate Professor in Department of Electronics and Communication Engineering, Ajay Kumar Garg Engineering College, Ghaziabad, India. His research interests include medical image processing, digital signal processing and control systems.